0026-895X/11/7901-185–196$20.00
MOLECULAR PHARMACOLOGY
Copyright © 2011 The American Society for Pharmacology and Experimental Therapeutics
Mol Pharmacol 79:185–196, 2011

Vol. 79, No. 1
69062/3654277
Printed in U.S.A.

Iron Chelators of the Di-2-pyridylketone Thiosemicarbazone and 2-Benzoylpyridine Thiosemicarbazone Series Inhibit HIV-1 Transcription: Identification of Novel Cellular Targets—Iron, Cyclin-Dependent Kinase (CDK) 2, and CDK9[S]

Zufan Debebe, Tatyana Ammosova, Denitra Breuer, David B. Lovejoy, Danuta S. Kalinowski, Pradeep K. Karla, Krishna Kumar, Marina Jerebtsova, Patricio Ray, Fatah Kashanchi, Victor R. Gordeuk, Des R. Richardson, and Sergei Nekhai

Center for Sickle Cell Disease, Department of Medicine (Z.D., T.A., D.B., V.R.G., S.N.) and Departments of Pharmaceutical Sciences (Z.D., P.K.K., K.K.) and Microbiology (D.B., S.N.), Howard University, Washington DC; Iron Metabolism and Chelation Program, Department of Pathology and Bosch Institute, University of Sydney, Sydney, Australia (D.B.L., D.S.K., D.R.R.); Children's National Medical Center, Washington DC (M.J., P.R.); and National Center for Biodefense and Infectious Diseases, George Mason University, Manassas, Virginia (F.K.)

Received September 26, 2010; accepted October 18, 2010

ABSTRACT

HIV-1 transcription is activated by HIV-1 Tat protein, which recruits cyclin-dependent kinase 9 (CDK9)/cyclin T1 and other host transcriptional coactivators to the *HIV-1* promoter. Tat itself is phosphorylated by CDK2, and inhibition of CDK2 by small interfering RNA, the iron chelator 2-hydroxy-1-naphthylaldehyde isonicotinoyl hydrazone (*311*), and the iron chelator deferasirox (ICL670) inhibits HIV-1 transcription. Here we have analyzed a group of novel di-2-pyridylketone thiosemicarbazone- and 2-benzoylpyridine thiosemicarbazone-based iron chelators that exhibit marked anticancer activity in vitro and in vivo (*Proc Natl Acad Sci USA* **103:**7670–7675, 2006; *J Med Chem* **50:**3716–3729, 2007). Several of these iron chelators, in particular 2-benzoylpyridine 4-allyl-3-thiosemicarbazone (Bp4aT) and 2-benzoylpyridine 4-ethyl-3-thiosemicarbazone (Bp4eT), inhibited HIV-1 transcription and replication at much lower concentrations than did 311 and ICL670. Neither Bp4aT nor Bp4eT were toxic after a 24-h incubation. However, longer incubations for 48 h or 72 h resulted in cytotoxicity. Analysis of the molecular mechanism of HIV-1 inhibition showed that the novel iron chelators inhibited basal HIV-1 transcription, but not the nuclear factor-κB-dependent transcription or transcription from an *HIV-1* promoter with inactivated SP1 sites. The chelators inhibited the activities of CDK2 and CDK9/cyclin T1, suggesting that inhibition of CDK9 may contribute to the inhibition of HIV-1 transcription. Our study suggests the potential usefulness of Bp4aT or Bp4eT in antiretroviral regimens, particularly where resistance to standard treatment occurs.

Introduction

Increased iron stores are correlated with faster HIV-1 progression in iron-loaded patients with thalassemia major, in patients infected with HIV administered with oral iron, and in those with the haptoglobin 2–2 polymorphism (Gordeuk et al., 2001). Moreover, a retrospective study of bone marrow macrophage iron in patients infected with HIV suggested that survival was inversely correlated with higher iron stores (Gordeuk et al., 2001).

Iron chelation therapy has been considered for the control of various infections such as those mediated by protozoa or intracellular pathogens (Hershko, 1994). Several studies have demonstrated the potential of iron chelators in inhibiting HIV replication (Georgiou et al., 2000, 2002; Traoré and Meyer, 2004). In cultured T cells, excess iron stimulates HIV-1 viral replication, whereas iron chelation with desferrioxamine (DFO) lowers viral replication, as measured by decreased p24 levels and reverse transcriptase (RT) activity (Traoré and Meyer, 2004). Treatment of monocyte-derived macrophages and peripheral blood lymphocytes with one of two chelators (DFO or deferiprone) reduced p24 expression

This project was supported by the National Institutes of Health National Heart, Lung, and Blood Institute and Office of Research on Minority Health [Grants 2R25-HL003679-08,R-1-HL55605, F31-HL090025]; the National Institutes of Health National Center for Research Resources [Grant 2M01-RR10284]; the National Institutes of Health National Institute of General Medical Sciences [1SC1-GM082325]; the National Institutes of Health Research Centers in Minority Institutions (RCMI) Program of the Division of Research Infrastructure, National Center for Research Resources [Grant 2G12-RR003048]; the National Institutes of Health National Institute of Diabetes and Digestive and Kidney Diseases [R01-DK49419]; the National Institutes of Health National Center for Complimentary and Alternative Medicine [R21AT002278]; and by the National Health and Medical Research Council of Australia [Senior Principal Research Fellowship 571123, Project Grant 570952].

D.R.R. and S.N. should be considered co-senior authors of this article and contributed equally to this work.

Article, publication date, and citation information can be found at http://molpharm.aspetjournals.org.

doi:10.1124/mol.110.069062.

[S] The online version of this article (available at http://molpharm.aspetjournals.org) contains supplemental material.

and inhibited cellular proliferation (Georgiou et al., 2000). The orally active bidentate chelators 1,6-dimethyl-3-hydroxy-4-(1*H*)-pyridinone-2-carboxy-(*N*-methyl)-amide hydrochloride (CP502) and 6-dimethyl-3-hydroxy-4-(1*H*)-pyridinone-2-carboxy-(*N*-methyl)-amide hydrochloride (CP511) decreased HIV-1 replication and cellular proliferation in a manner similar to that of DFO and deferiprone (Georgiou et al., 2002). Thus, the observed reduction of HIV-1 replication by these chelators may reflect inhibition of cellular proliferation rather than inhibition of a specific host cell factor involved in HIV-1 replication.

In our previous study, HIV-1 transcription was inhibited in CEM T cells by the tridentate iron chelators 2-hydroxy-1-naphthylaldehyde isonicotinoyl hydrazone (311; IC_{50} = 2 μM) and ICL670 (also known as deferasirox; IC_{50} = 23 μM) (Debebe et al., 2007). These iron chelators inhibited the cellular activity of cyclin-dependent kinase (CDK) 2 (Debebe et al., 2007). Although ICL670 has been recently approved for clinical use in the United States and has been successfully implemented for the treatment of iron overload (Porter, 2006), the relatively high concentrations of ICL670 needed for the inhibition of HIV-1 were of concern. The iron chelator 311 was shown to be cytotoxic at low micromolar concentrations (IC_{50} = 3 μM) (Becker et al., 2003). Hence, the inhibition of HIV-1 that we observed with 311 may be related in part to the inhibition of DNA synthesis and cellular proliferation.

The goal of the present study was to screen and identify novel iron chelators that would be more potent inhibitors of HIV-1 transcription than ICL670 or equally inhibitory but less cytotoxic than 311. We also were interested to determine whether inhibition of HIV-1 transcription was due to the inhibition of CDK9/cyclin T1, a major RNA polymerase II kinase that interacts with HIV-1 Tat and induces HIV-1 transcription (Nekhai and Jeang, 2006). For this purpose, we examined a library of di-2-pyridylketone thiosemicarbazone (DpT) and 2-benzoylpyridine thiosemicarbazone (BpT)-based tridentate iron chelators (Fig. 1A) (Yuan et al., 2004; Whitnall et al., 2006; Kalinowski et al., 2007). The DpT chelators, especially di-2-pyridylketone 4,4-dimethyl-3-thiosemicarbazone (Dp44mT), have been shown to have potent antitumor activity in vitro and in vivo (Yuan et al., 2004; Whitnall et al., 2006). It is noteworthy that mice treated with optimal Dp44mT showed little alteration in hematological and biochemical indices at the chelator doses (0.4 mg/kg/day) required to induce antitumor activity (Whitnall et al., 2006). The BpT-based iron chelators exhibited comparable antineoplastic activity than their DpT homologs in vitro and are among the most active anticancer agents developed by Richardson and colleagues (Kalinowski et al., 2007).

In the current investigation, we identified the two most potent inhibitors of HIV-1 from the BpT and DpT series of chelators and discovered novel molecular mechanisms involved in their activity. Utilization of these new iron-chelating agents in treatment schedules could be of clinical significance in patients with HIV who are resistant to current antiviral treatment regimens.

Materials and Methods

Materials. 293T and CEM T cells were purchased from the American Type Culture Collection (Manassas, VA). The CEM-HIV-1 [long terminal repeat (LTR)] GFP cells (courtesy of Dr. Jacques Corbeil, Centre de Recherche en Infectiologie du CHUL, Québec, QC, Canada) and OM10.1 cells (courtesy of Dr. Salvatore Butera, Retrovirus Diseases Branch, DVRD/NCID, Centers for Disease Control and Prevention, Atlanta, GA) were obtained from the National Institutes of Health AIDS Research and Reference Reagent Program. Histone H1 was purchased from Millipore (Billerica, MA). Anti-FLAG monoclonal antibody, protein G, and protein A agarose were purchased from Sigma (St. Louis, MO). All radioactive reagents were purchased from GE Healthcare (Chalfont St. Giles, Buckinghamshire, UK). Antibodies against CDK9, CDK2, and cyclin T1 were purchased from Santa Cruz Biotechnology (Santa Cruz, CA). Horseradish peroxidase-conjugated $F(ab)_2$ fragment was purchased from GE Healthcare. All other inorganic reagents were purchased from Thermo Fisher Scientific (Waltham, MA) or Sigma. Roscovitin was purchased from Calbiochem (La Jolla, CA), and 4-amino-6-hydrazino-7-β-D-ribofuranosyl-7*H*-pyrrolo[2,3-*d*]-pyrimidine-5-carboxamide (ARC) was a gift from Dr. Andrei Gartel (University of Illinois, Chicago, IL).

Chelators. All chelators were synthesized by Schiff base condensation between the relevant aromatic ketone or aldehyde with a thiosemicarbazide or acid hydrazide using standard methods (Kalinowski et al., 2007). The chelators were characterized using a combination of elemental analysis, ^{1}H NMR spectroscopy, infrared spectroscopy, and mass spectroscopy.

Cell Culture. All cells were cultured at 37°C in a 5% CO_2 atmosphere. CEM T cells and peripheral-blood mononuclear cells (PBMCs) were cultured in RPMI 1640 medium (Invitrogen, Carlsbad, CA) containing 10% fetal bovine serum, and 1% antibiotic solution (penicillin and streptomycin; Invitrogen). CEM GFP cells were cultured in RPMI 1640 medium with all the additions above plus 500 μg/ml G418 (Invitrogen). The 293T cells and OM10.1 cells were cultured in Dulbecco's modified Eagle's medium (Invitrogen) containing 10% fetal bovine serum and 1% antibiotic solution (penicillin and streptomycin).

Induction of HIV-1 Transcription with Adenovirus Carrying Tat. The E1-deleted recombinant adenovirus carrying Tat was generated as described previously (Debebe et al., 2007). In brief, CEM-GFP cells were infected in 96-well plates containing 4×10^5 cells/well. After 24 h at 37°C, 10-μl aliquots were removed, supplemented with trypan blue, and counted to determine cellular viability. The remaining cells were transferred to a white plate (PerkinElmer Life and Analytical Sciences, Waltham, MA), and fluorescence was measured at an excitation wavelength of 488 nm and an emission

ABBREVIATIONS: DFO, desferrioxamine; RT, reverse transcriptase; CP502, 1,6-dimethyl-3-hydroxy-4-(1*H*)-pyridinone-2-carboxy-(*N*-methyl)-amide hydrochloride; 311, 2-hydroxy-1-naphthylaldehyde isonicotinoyl hydrazone; ICL670, deferasirox; CDK, cyclin-dependent kinase; DpT, di-2-pyridylketone thiosemicarbazone; BpT, 2-benzoylpyridine thiosemicarbazone; Dp44mT, di-2-pyridylketone 4,4-dimethyl-3-thiosemicarbazone; LTR, long terminal repeat; GFP, green fluorescent protein; ARC, 4-amino-6-hydrazino-7-β-D-ribofuranosyl-7*H*-pyrrolo[2,3-*d*]-pyrimidine-5-carboxamide; PBMC, peripheral blood mononuclear cell; NF-κB, nuclear factor-κB; WT, wild type; ONPG, *o*-nitrophenyl-β-D-galactopyranoside; AM, acetoxymethyl ester; PI, propidium iodide; DTT, dithiothreitol; CMV, cytomegalovirus; EGFP, enhanced green fluorescent protein; PVDF, polyvinylidene difluoride; PAGE, polyacrylamide gel electrophoresis; CTD, C-terminal domain; LS, low salt; HS, high salt; Dp2mT, di-2-pyridylketone 2-methyl-3-thiosemicarbazone; Bp44mT, 2-benzoylpyridine 4,4-dimethyl-3-thiosemicarbazone; Bp4eT, 2-benzoylpyridine 4-ethyl-3-thiosemicarbazone; Bp4aT, 2-benzoylpyridine 4-allyl-3-thiosemicarbazone; Bp4pT, 2-benzoylpyridine 4-phenyl-3-thiosemicarbazone; CP511, 6-dimethyl-3-hydroxy-4-(1*H*)-pyridinone-2-carboxy-(*N*-methyl)-amide hydrochloride; PKTBH, di-2-pyridylketone thiobenzoyl hydrazone; CTDo, hyperphosphorylated C-terminal domain of RNA polymerase II; CTDa, hypophosphorylated C-terminal domain of RNA polymerase II; eIF5α, host elongation factor 5A.

wavelength of 510 nm by using a luminescence spectrometer (LS50B; PerkinElmer Life and Analytical Sciences).

Data Analysis. Cytotoxicity data are presented as a percentage of the control versus logarithm of the chelator concentration and analyzed using Prism software (ver. 3; GraphPad Software, La Jolla, CA). The IC_{50} values were determined from the dose-response (variable slope) curve using a four parameter logistic equation: $Y = \text{Bottom} + (\text{Top} - \text{Bottom})/(1 + 10^{((\log EC_{50} - X) \times n_H)})$, where

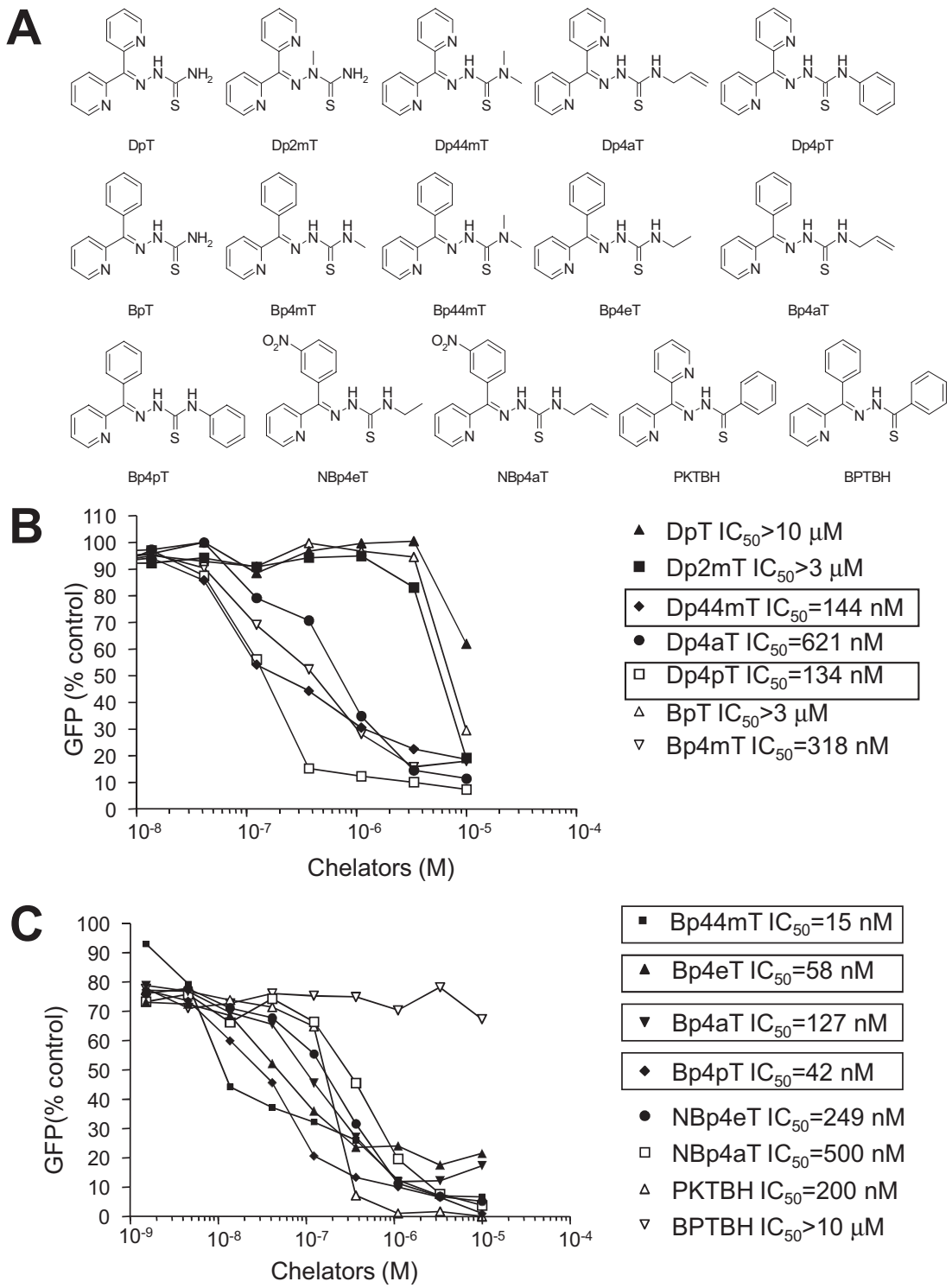

Fig. 1. Structures of the chelators used in this study (A) and the effect of DpT- and BpT-based iron chelators on HIV-1 transcription (B and C) in CEM GFP cells. A, chemical structures of the iron chelators examined in this study, including members of the DpT series, BpT series, 2-(3-nitrobenzoyl) pyridine thiosemicarbazone (NBpT) series, di-2-pyridylketone thiobenzoyl hydrazone (PKTBH), and 2-benzoylpyridine thiobenzoyl hydrazone (BPTBH). B and C, inhibition of HIV-1 transcription in CEM-GFP cells. CEM-GFP cells were infected with adenovirus carrying Tat and then incubated with the indicated chelators for 24 h at 37°C. GFP fluorescence was measured in live cells. B and C, show different iron chelators that were separated into two graphs for clarity. The chelators enclosed in boxes were those with the lowest IC_{50} values for inhibition of HIV-1 transcription. IC_{50} values were determined using Prism 3 software as described under *Materials and Methods.* Results are means of three independent experiments.

Y is a percentage of the control, X is logarithm of the chelator concentration, and n_H is Hill slope.

Plasmids. The HIV-1 reporter containing HIV-1 LTR (−138 to +82) followed by a nuclear localization signal and the *LacZ* reporter gene (courtesy of Dr. Michael Emmerman, Fred Hutchinson Cancer Institute, Seattle, WA) and the pNL4-3.Luc.R$^-$E$^-$ (courtesy of Prof. Nathaniel Landau, New York University School of Medicine, New York, NY) were obtained from the National Institutes of Health AIDS Research and Reference Reagent Program. The NF-κB driven *e-selectin-luciferase* reporter was a gift from Dr. Chou-Zen Giam (Uniformed Services University of the Health Sciences, Bethesda, Maryland) (Fu et al., 2003). The following plasmids were kindly provided by Dr. Manuel López-Cabrera (Unidad de Biología Molecular, Madrid, Spain): WT HIV-1 LTR (−105– +77) followed by the *luciferase* reporter gene (WT SP KB); HIV-1 (−105– +77) with Sp1-inactivated sites followed by the *luciferase* reporter gene (WT SP 123); and HIV-1 (−81– +77) with NF-κB-deleted sites followed by the *luciferase* reporter gene (WT SP).

Transient Transfections. 293T cells were cotransfected with Tat-expressing vector and HIV-1 LTR-*LacZ* at 30% confluence using Lipofectamine and Plus reagents (Invitrogen). After transfection, the cells were cultured for an additional 48 h at 37°C, and β-galactosidase activity was analyzed with the use of the quantitative *o*-nitrophenyl-β-D-galactopyranoside (ONPG)-based assay (see next section) (Debebe et al., 2007).

β-Galactosidase Assays. Cells were washed with PBS and lysed for 20 min at room temperature in 50 μl of lysis buffer containing 20 mM HEPES at pH 7.9, 0.1% Tergitol-type NP-40 (NP-40), and 5 mM EDTA. Subsequently, 100 μl of ONPG solution (72 mM Na_2PO_4 at pH 7.5, 1 mg/ml ONPG, 12 mM $MgCl_2$, and 180 mM 2-mercaptoethanol) was added and incubated at room temperature. Standards were incubated for 10 min. Based on the linear part of the standard curve, the color development was monitored and stopped when the signal was in the middle of the linear range. The reaction was terminated by the addition of 100 μl of 1 M Na_2CO_3. The 96-well plate was analyzed in a microplate reader at 414 nm (Multiskan MS; Thermo Fisher Scientific).

Cell Viability Assays (Propidium Iodide Uptake, Calcein-AM Uptake, and Trypan Blue Exclusion Assay). CEM T cells were grown in 96-well plates at 37°C and incubated with iron chelators for the periods of time indicated in the figure legends. To measure toxicity by propidium iodide (PI; Sigma) uptake, PI (250 μg/ml) was incubated with cells for 30 min at 37°C. PI fluorescence was measured at an excitation and emission wavelengths of 488 and 617 nm, respectively, by using the luminescence spectrometer described above.

To assess cytotoxicity with calcein, media was removed and the cells were washed with Dulbecco's PBS to remove serum esterase activity that may cause an increase in fluorescence through the hydrolysis of calcein-AM. Cells were then supplemented with 0.2 μM calcein-AM (Invitrogen) for 10 min at 37°C. A positive control containing 100% dead cells was prepared by treating cells with Triton X-100 [1% (v/v)] that were then incubated with 0.2 μM calcein-AM. Fluorescence was measured using the luminescence spectrometer described above implementing an excitation wavelength of 495 nm and emission filters at 515 nm. To measure cellular viability, the cells were supplemented with 0.2% trypan blue, transferred to a plastic disposable counting chamber and counted on a Cellometer Automatic Cell Counter (Nexcelcom Bioscience, Lawrence, MA).

Preparation of Pseudotyped HIV-1 Expressing Luciferase. 293T cells were grown on 100-mm plates at 37°C and transfected using the calcium phosphate method. Cells were transfected with the VSVG-expressing vector (gpHEF-VSVG) and pNL4-3.Luc.R$^-$E$^-$ molecular clone that contains two nonsense frame shifts in the *Env* and *Vpr* genes. In this vector, the *luciferase* gene was cloned in place of *nef* (He and Landau, 1995). Seventy-two hours after transfection, the media were collected and briefly centrifuged at 1000*g* for 10 min, and the virus was collected by centrifugation at 4°C for 6 h at 14,000*g*. The precipitated virus was resuspended in PBS containing 10% glycerol, separated into aliquots, and stored at −70°C. The p24 analysis of the HIV-1 Luc was performed by enzyme-linked immunosorbent assay using a kit from ZeptoMetrix (Buffalo, NY).

Luciferase Assay. CEM T cells were infected with VSVG-pseudotyped pNL4-3.Luc.R$^-$E$^-$ virus and then cultured at 0.5×10^6 cells/ml in six-well plates at 37°C and 5% CO_2. The cells were collected, washed with PBS, and resuspended in 100 μl of PBS. Then, 100 μl of reconstituted luciferase buffer (Luclite Kit; PerkinElmer Life and Analytical Sciences) was added to each well. After a 10-min incubation, the lysates were transferred into white plates (PerkinElmer Life and Analytical Sciences), and luminescence was measured using LuminoSkan RT equipment (Thermo Fisher Scientific).

Source of PBMCs. PBMCs were purchased from Astarte Biologics (Redmond, WA). Donors were negative for HIV-1 and -2, hepatitis B, hepatitis C, and human T-lymphotropic virus type 1. PBMCs were isolated from peripheral blood by apheresis with additional purification by density gradient centrifugation and then cryopreserved until used.

Infection of PBMCs with VSVG HIV-Luc and Inhibition of HIV-1 with Iron Chelators. PBMCs were infected with HIV-1 Luc virus at approximately 1 ng of p24 per 5×10^6 cells. After 48 h, the cells were seeded on 96-well white plates and incubated with the iron chelators for 24 h at 37°C. Luciferase buffer was then added to each well, and luminescence was measured using Luminoskan RT equipment as described under *Luciferase Assay*.

Viability of PBMCs after Iron Chelator Treatment. PBMCs were grown on a 96-well white plate and incubated with the iron chelators for different time periods at 37°C. Later, cells were washed with PBS and incubated with 0.2 μM calcein-AM for 15 min, and fluorescence was measured at an excitation wavelength of 495 nm and an emission wavelength of 515 nm using Luminescence Spectrometer LS 50B (PerkinElmer Life and Analytical Sciences). Values presented are mean ± S.D. ($n = 4$) and are typical of three independent experiments.

Inhibition of HIV-1 Replication Using Iron Chelators. In these studies, OM10.1 cells were used where the integrated HIV-1 proviral DNA was originally derived from the subtype B, LAI strain (Butera et al., 1994). To assess the activity of chelators on inhibiting HIV-1 replication, 10^6 OM10.1 cells were grown to 70% confluence and treated with 10 ng/ml TNF-α for 2 h at 37°C. Subsequently, TNF-α was removed, and the cells were washed with PBS and then treated with the concentrations of iron chelators indicated in the figure legends. Media was collected 48 h after the drug treatment, and the activity of RT was determined. Viral supernatants (10 μl) were incubated in a 96-well plate with RT reaction mixture containing 1× RT buffer (50 mM Tris-HCl, 1 mM DTT, 5 mM $MgCl_2$, and 20 mM KCl), 0.1% Triton X-100, 0.01 units of poly(A), 0.01 units of poly(dT), and [^{3}H]TTP. The mixture was incubated overnight at 37°C, and 5 μl of the reaction mix was spotted on a DEAE Filtermat (PerkinElmer Life and Analytical Sciences), washed four times with 5% Na_2HPO_4 and three times with water, and then dried completely. RT activity was measured using a Betaplate counter (PerkinElmer Life and Analytical Sciences).

Analysis of the NF-κB-Driven E-Selectin-Luciferase Reporter Activity. 293T cells were seeded at 30% confluence in 96-well plates and allowed to grow overnight. The following day, the cells were transfected with CMV-EGFP reporter in combination with the NF-κB driven *e-selectin-luciferase* reporter (Fu et al., 2003), or pNL4-3.Luc.R$^-$E$^-$ (*HIV-1* promoter) for 3 h at 37°C using Lipofectamine and then incubated with Bp4aT or Bp4eT for 48 h at 37°C. The media were then removed from the cells, and equal amounts of PBS and luciferase buffer were added to measure luciferase activity. After luciferase activity, GFP was measured at an excitation wavelength of 495 nm and an emission wavelength of 515 nm.

Analysis of HIV-1 Promoters with the Deletion of NF-κB and Inactivation of Sp1 sites. 293T cells were transfected at 30%

confluence in 96-well plates with vectors in which the *luciferase* reporter was driven by WT HIV-1 LTR (−105 to +77), HIV-1 LTR (−105 to +77), with Sp1-inactivated sites or HIV-1 LTR (−81 to +77) with NF-κB-deleted sites (courtesy of Dr. Manuel López-Cabrera, Unidad de Biología Molecular, Madrid, Spain). The cells were transfected for 3 h at 37°C using Lipofectamine Plus and then incubated with iron chelators or control medium for 18 h at 37°C. The media was then removed from the cells and equal amounts of 1× PBS and luciferase buffer were added to measure luciferase activity.

Immunoblots and Kinase Assay. 293T cells were incubated with control medium or control medium containing chelators and incubated for 24 h at 37°C. Cells were then washed with PBS, and whole-cell lysates were prepared from the cells using whole-cell lysis buffer (50 mM Tris-HCl, pH 7.5, 0.5 M NaCl, 1% NP-40, and 0.1% SDS) supplemented with antiprotease cocktail (Sigma). Protein concentration of the lysates was measured by the Bradford assay (Bio-Rad Laboratories, Hercules, CA) and 30 to 50 μg of total protein was subjected to electrophoresis using 10% SDS-PAGE. The gels were transferred onto a polyvinylidene fluoride (PVDF) membrane (Millipore) and analyzed for CDK2, CDK9, and cyclin T1. The blots were developed and quantified using a ChemiDoc XRS Station (Bio-Rad Laboratories). Immunoprecipitation assays were carried out with 400 μg of the cell lysate and 800 ng of antibody combined with 50 μl of a 50% slurry of protein A agarose for 2 h at 4°C in TNN buffer (50 mM Tris-HCl, pH 7.5, 0.15 M NaCl, and 1% NP-40). The agarose beads were precipitated, washed with TNN buffer, and divided into two parts and used for the kinase assay and Western blotting. The kinase assay was performed at 30°C for 30 min in a kinase assay buffer (50 mM HEPES-KOH, pH 7.9, 10 mM $MgCl_2$, 6 mM EGTA, and 2.5 mM DTT) containing 1 μg of histone H1 as a substrate, 200 μM ATP, and 5 μCi of [γ-^{32}P]ATP.

C-Terminal Domain of RNA Polymerase II Phosphorylation Assay. The CTD phosphorylation assay was performed at 30°C for 30 min in 20 μl of kinase assay buffer (50 mM HEPES-KOH, pH 7.9, 10 mM $MgCl_2$, 6 mM EGTA, and 2.5 mM DTT) containing 4 μg of CTD substrate, 250 μM ATP, and 5 μCi of [γ-^{32}P]ATP. Recombinant CDK2/cyclin E or CDK9/cyclin T1 were used as controls. The reaction was stopped with SDS-loading buffer and resolved using 10% PAGE. The dried gel was subjected to filmless autoradiographic analysis. In parallel, the products of immunoprecipitation were resolved using 10% Tris-glycine SDS-PAGE, transferred to PVDF membranes (Millipore), and immunoblotted with appropriate antibodies.

Separation of Large and Small CDK9/Cyclin T1-Containing Complexes by Differential Salt Extraction. We used a method developed by Biglione et al. (2007) to quantify the relative amounts of large and small CDK9/cyclin T1-containing complexes based on differential nuclear extraction. 293T cells were grown on six-well plates at 37°C and 5% CO_2 and then incubated with the iron chelators (1 μM) for 24 h at 37°C. Cells were then suspended in buffer A [10 mM HEPES, pH 7.9, 10 mM KCl, 10 mM $MgCl_2$, 1 mM EDTA, 250 μM sucrose, 1 mM DTT, 0.5% NP-40, and protease inhibitor cocktail (Sigma)] added at 500 μl/10^7 cells. The mixture was incubated on ice for 10 min and centrifuged at 1000*g* for 5 min to pellet the nucleus. The supernatant was removed and saved as the low-salt (LS) extract. The remaining pellet was resuspended in buffer B (20 mM HEPES-KOH, pH 7.9, 450 mM NaCl, 1.5 mM $MgCl_2$, 0.5 mM EDTA, 1 mM DTT, and protease inhibitor cocktail) added at 500 μl/10^7 cells. The mixture was incubated on ice for 10 min and centrifuged at 10,000*g* for 1 h at 4°C. The supernatant was collected as the high-salt (HS) extract and the pellet was discarded. The lysates were loaded on 10% polyacrylamide gel and transferred to PVDF membrane and western blotting analysis was performed for the expression of CDK9 and cyclin T1.

Statistical Analysis. Results were expressed as mean ± S.D. Data were compared using Student's *t* test. Results were considered significant when $p < 0.05$.

Results

Identification of Bp4aT and Bp4eT as the Most Efficient and Least Cytotoxic Inhibitors of HIV-1 Transcription. We analyzed 15 selected DpT and BpT-derived iron chelators, including a control nonchelating analog, Dp2mT, that was designed and characterized in previous studies (Yuan et al., 2004; Kalinowski et al., 2007) (Fig. 1A and Table 1). These agents were assessed using CEM-T cells containing an integrated HIV-1 LTR-GFP (CEM-GFP). HIV-1 transcription in CEM-GFP cells was induced by infection with adenovirus expressing Tat, and GFP fluorescence was measured to quantify viral transcription, as described previously (Debebe et al., 2007; Nekhai et al., 2007). Data were analyzed using Prism 3 software and showed that after a 24-h incubation of CEM T cells with the 15 chelators tested, 11 ligands inhibited HIV-1 transcription with submicromolar IC_{50} values (Table 1 and Fig. 1, B and C). The six most active chelators (IC_{50}<0.2 μM) were Dp44mT, Dp4pT, Bp44mT, Bp4eT, Bp4aT, and Bp4pT (Table 1). Bp44mT had the lowest IC_{50} for inhibition of HIV-1 transcription, namely 15 nM (Table 1 and Fig. 1C).

The short-term toxicity of the iron chelators was analyzed by propidium iodide uptake in the treated CEM T cells in comparison with the untreated control. As a positive control for cell death, untreated cells were lysed by the addition of the nonionic detergent, Triton X-100 [1% (v/v)]. Toxicity of the chelators and that of the noncytotoxic, nonchelating control compound Dp2mT (Yuan et al., 2004) were then analyzed. These results showed that Dp4pT, Bp44mT, Bp4pT, and di-2-pyridylketone thiobenzoyl hydrazone (PKTBH) were clearly cytotoxic over 24 h (see IC_{50} values in Table 1 and Supplemental Fig. 1). As shown previously, Dp2mT was not cytotoxic at concentrations below 10 μM, because it cannot bind cellular iron pools (Yuan et al., 2004).

Inhibition of One-Round HIV-1 Replication in CEM T Cells. Based on the results above, we selected Bp4aT and Bp4eT for further analysis as the most potent and least

TABLE 1

Effect of DpT- and BpT-based iron chelators on HIV-1 transcription and cytotoxicity over a 24-h incubation period

IC_{50} values were determined using Prism software. Results are mean values from three experiments.

Chelator	IC_{50}	
	Inhibition of HIV-1 Transcription, CEM T Cells	Cytotoxicity, CEM T Cells
	μM	
DpT	>10	>10
Dp2mT	>3	>10
Dp44mT	0.144	>10
Dp4aT	0.621	>10
Dp4pT	0.134	2.1
BpT	>3	>10
Bp4mT	0.318	>10
Bp44mT	0.015	2
Bp4eT	0.058	>10
Bp4aT	0.127	>10
Bp4pT	0.042	0.9
NBp4eT	0.249	>10
NBp4aT	0.500	>10
PKTBH	0.200	1.2
BPTBH	>10	>10

BPTBH, 2-benzoylpyridine thiobenzoyl hydrazone; NBp4eT, 2-(3-nitrobenzoyl) pyridine 4-ethyl-3-thiosemicarbazone; NBp4aT, 2-(3-nitrobenzoyl) pyridine 4-allyl-3-thiosemicarbazone.

cytotoxic compounds that inhibited HIV-1 transcription in 293T and CEM T cells. We analyzed the effect of Bp4aT and Bp4eT on one round of HIV-1 replication in comparison with the positive and negative controls, Bp4pT and BpT, which showed marked and little activity in inhibiting HIV-1 transcription, respectively (Table 1). In these experiments, CEM T cells were infected with pseudotyped HIV-1 virus containing luciferase in place of the *nef* gene (HIV-1 Luc) (He and Landau, 1995). CEM T cells were infected overnight with the virus and then cultured for 24 h at 37°C with or without the indicated concentration of chelators (Fig. 2A). In these experiments, Bp4eT was the most efficient inhibitor (IC_{50} = 75.0 ± 5.5 nM), followed by Bp4aT (IC_{50} = 160 ± 16 nM), Bp4pT (IC_{50} = 340 ± 53 nM), and BpT (IC_{50} = 1.60 ± 0.26 μM) (Fig. 2A).

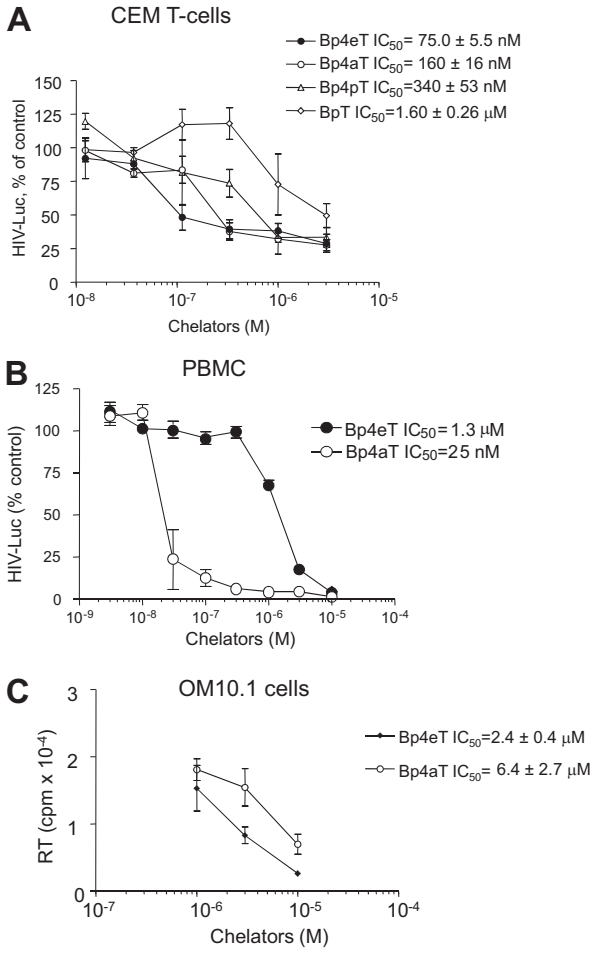

Fig. 2. Effect of chelators on HIV-1 replication. A, effect of chelators on one round of HIV-1-Luc replication in CEM T cells. CEM T cells were infected with VSVG-pseudotyped pNL4-3.Luc.R^-E^- (HIV-1 Luc) virus for 18 h at 37°C and then incubated for 24 h at 37°C with the indicated concentrations of iron chelators as shown in the figure. Luciferase activity was then measured and values presented as mean ± S.D. (n = 4) in a typical experiment of three independent experiments performed. IC_{50} values were determined using Prism 3 software. B, anti-HIV-1 activity of Bp4aT and Bp4eT in PBMCs infected with pseudotype HIV-1-Luc. PBMCs were infected with VSVG-pseudotyped HIV-1 Luc virus. After 48 h at 37°C, cells were seeded on 96-well plates and incubated with the chelators at the indicated concentrations for 24 h at 37°C. Later, luciferase buffer was added to each well and luciferase activity was measured. IC_{50} values were determined using Prism 3 software. C, inhibition of HIV-1 replication in OM10.1 cells by Bp4aT and Bp4eT. HIV-1 replication was induced in OM10.1 cells as described under *Materials and Methods*, and the cells were subsequently treated with the indicated concentrations of Bp4aT or Bp4eT for 48 h at 37°C. Media was collected and the activity of reverse transcriptase determined as described under *Materials and Methods*. Values presented are mean ± S.D. (n = 3) in a typical experiment of three performed.

Inhibition of One-Round HIV-1 Replication in PBMCs. We also analyzed the effect of Bp4aT and Bp4eT on one round of HIV-1 replication in PBMCs in comparison with BpT. PBMCs were infected with pseudotyped HIV-1 Luc virus for 48 h at 37°C and then cultured for 24 h at 37°C with or without the indicated concentration of chelators (Fig. 2B). In these cells, only Bp4aT markedly inhibited luciferase activity with an IC_{50} = 25 nM, whereas Bp4eT inhibited HIV-1 replication at a much higher concentration (IC_{50} = 1.3 μM; Fig. 2B).

Inhibition of HIV-1 Replication in OM10.1 Cells. Considering the effective antiviral activity observed above on HIV-1 transcription or one-round HIV-1 replication, it was important to compare the efficacy of these chelators on productive HIV-1 replication. To perform these studies, we used HIV-1-infected OM10.1 cells that were treated with TNF-α to analyze the inhibitory effects of iron chelators. Both Bp4eT and Bp4aT inhibited HIV-1 replication, the IC_{50} being 2.4 ± 0.4 and 6.4 ± 2.7 μM, respectively (Fig. 2C). Thus, the chelators were also able to inhibit productive HIV-1 replication.

Comparison of the Inhibition of HIV-1 Transcription by Bp4aT and Bp4eT with That of ARC and Roscovitin. Considering the effective antiviral activity of Bp4eT and Bp4aT, it was important to compare the efficacy of these chelators with known HIV-1 transcription inhibitors. We compared inhibition of HIV-1 transcription in 293T cells

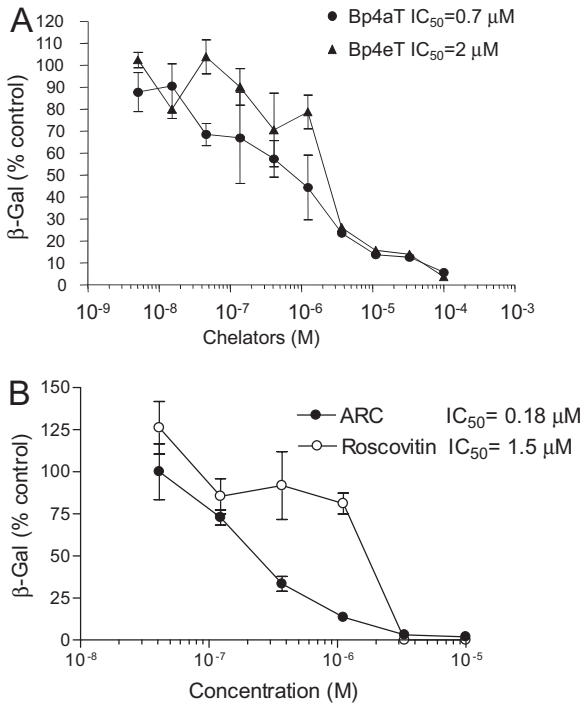

Fig. 3. Inhibition of Tat-induced HIV-1 transcription using 293T cells by iron chelators and CDK9 and CDK2 inhibitors ARC and roscovitin. 293T cells were transfected with HIV-1 LTR-Lac Z, CMV-EGFP, and Tat-expression vectors and then incubated with the indicated concentrations of iron chelators (A) or the CDK9 and CDK2 inhibitor ARC or roscovitin (B) for 24 h at 37°C. HIV-1 transcription was analyzed by measuring β-galactosidase activity. The results are mean ± S.D. (n = 4) and are typical of three independent experiments. The IC_{50} values were calculated using Prism 3 software.

transfected with HIV-1 LTR-LacZ and Tat expression vectors. Bp4aT and Bp4eT inhibited Tat-induced HIV-1 transcription in 293T cells at low micromolar concentrations (Fig. 3A). To compare the effect of the iron chelators with the effect of known HIV-1 transcription inhibitors, we incubated these transfected cells with ARC or roscovitin, which inhibit HIV-1 transcription through the deregulation of CDK9 and CDK2, respectively (for review, see Nekhai and Jeang, 2006). After a 24-h incubation at 37°C, HIV-1 transcription was inhibited by ARC (IC_{50} = 180 nM) and by roscovitin (IC_{50} = 1.5 μM) (Fig. 3B). Thus, the iron chelators, Bp4aT and Bp4eT, were approximately 4- to 16-fold less efficient inhibitors of HIV-1 than ARC but were comparable to roscovitin. However, it is relevant to note that these chelators have not been specifically designed as antiviral agents, and their potential may lie in their novel mechanism of action (examined under *Inhibition of CDK9*).

Toxicity of Iron Chelators. Analysis of short-term cytotoxicity of Bp4aT and Bp4eT was performed in comparison with the negative control chelator, BpT, which showed little toxicity after 24 h (Table 1). In these studies using calcein-AM uptake (Papadopoulos et al., 1994), the chelators were demonstrated to be equally nontoxic after a 24-h incubation period (IC_{50} >100 μM; Fig. 4A). We further analyzed long-term cytotoxicity of Bp4aT and Bp4eT in comparison with the negative control BpT in CEM T cells after 1 to 5 days of incubation implementing the calcein-AM assay. The number of viable cells decreased after 2-day treatment and remained low for up to 5 days of incubation (Fig. 4B). Analysis of cell growth using the trypan blue viability assay showed that although control cells continued to grow, cells in the presence of chelators did not proliferate (Supplemental Fig. 2A). Analysis of the long-term cytotoxicity of Bp4aT, Bp4eT, and BpT in PBMCs at 0.3 μM showed that Bp4aT was more toxic compared with Bp4eT or BpT (Fig. 4C). These results showed that although iron chelators were not toxic during the 24-h incubation when the antiviral effect was observed, longer incubation times demonstrated cytotoxicity. Taken together, the results above demonstrated that among the analyzed iron chelators, Bp4eT was the most promising antiviral agent.

Examination of the Effect of Chelators on Sp1- and NF-κB-Driven Transcription. Sp1 activity is important for HIV-1 basal transcription (Jochmann et al., 2009) and Tat-induced HIV-1 transcription (Chun et al., 1998). NF-κB is activated in various cell types in response to hypoxia and is important for Tat-activated HIV-1 transcription, because it acts in concert with Tat and CDK9/cyclin T1 (West et al., 2001). Considering this, to determine whether iron chelators have an effect on NF-κB- and Sp1-driven activity, we analyzed their effect on the NF-κB-dependent *e-selectin* promoter as a relevant positive control (Fu et al., 2003). This was then compared with the effects of the chelators on the activity of *HIV-1* promoters with the deletion of NF-κB sites or inactivation of Sp1 sites in 293T cells (Gómez-Gonzalo et al., 2001). Bp4eT at 10 μM inhibited the activity of WT HIV-1 LTR in the HIV-1 proviral pNL4-3.Luc.R^-E^- (pNL-Luc) promoter in 293T cells (Fig. 5A). In contrast, the activity of the NF-κB-dependent *e-selectin* promoter (Fu et al., 2003) was not affected in 293T cells incubated with this chelator (Fig. 5A). This suggested that NF-κB activity was not changed after incubation of cells with iron chelators. It should be noted that analysis of cytotoxicity in 293T cells by the calcein-AM uptake assay showed that Bp4eT (10 μM) did not exhibit significant toxicity compared with the control after 24 h (Supplemental Fig. 2B).

In the absence of Tat, basal activity of the WT HIV-1 LTR promoter (denoted WT SP KB) was reduced by 2.7-fold in 293T cells incubated with 10 μM Bp4eT (Fig. 5B). In contrast, the activities of the HIV-1 LTR without NF-κB sites (WT SP) or with inactivated Sp1 sites (WT SP 123) were reduced by only 1.3- and 1.4-fold, respectively (Fig. 5B). These results indicated that inactivation of Sp1 sites or de-

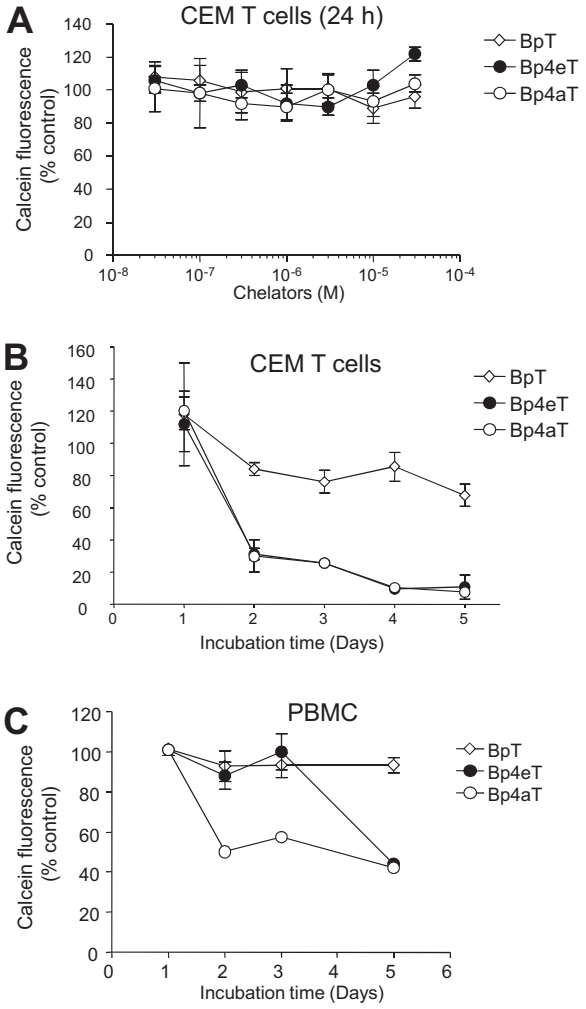

Fig. 4. Effect of iron chelators on viability of CEM T cells and PBMCs. A, short- term effect of Bp4aT and Bp4eT on the viability of CEM T cells. CEM T cells were incubated with the indicated concentrations of the chelators for 24 h at 37°C. The cells were then washed with PBS and incubated with 0.2 μM calcein-AM for 15 min at 37°C, and fluorescence was measured at an excitation wavelength of 495 nm and an emission wavelength of 515 nm. Values presented are mean ± S.D. (n = 4) and are typical of 3 independent experiments. B, long-term effect of Bp4aT and Bp4eT on the viability of CEM T cells. CEM T cells were incubated with Bp4aT, Bp4eT, and BpT at 10 μM for 24, 48, 72, 96, and 120 h at 37°C. The cells were then washed with PBS and incubated with 0.2 μM calcein-AM for 15 min at 37°C, and fluorescence was measured at an excitation wavelength of 495 nm and an emission wavelength of 515 nm. Values presented are mean ± S.D. (n = 4) and are typical of three independent experiments. C, long-term effect of Bp4aT and Bp4eT on the viability of PBMC. PBMC cells were incubated with the iron chelators (0.3 μM) for the indicated number of days at 37°C. Cells were then washed with PBS and incubated with 0.2 μM calcein-AM for 15 min at 37°C, and fluorescence was measured at an excitation wavelength of 495 nm and an emission wavelength of 515 nm. Values presented are mean ± S.D. (n = 4) and are typical of three independent experiments.

letion of NF-κB sites makes the remaining promoter activity less sensitive to Bp4eT. Thus, the effect of the iron chelators on basal HIV-1 transcription might involve deregulation of a factor other than Sp1 or NF-κB. Other possible factors that could be affected by the chelators include CDK9/cyclin T1, and this is assessed under *Inhibition of CDK9*.

Inhibition of CDK2. We have demonstrated previously that 311 and ICL670 inhibited CDK2 activity (Debebe et al., 2007). To determine whether the most effective BpT and DpT chelators had a similar effect, CDK2 was immunoprecipitated from 293T cells incubated for 24 h at 37°C with Dp44mT, Bp4aT, or Bp4eT and also the positive control chelator 311 or ICL670 (all at 10 μM except ICL670, which was used at 100 μM because of its low efficacy; Fig. 6A). These studies showed that Bp4eT, Dp44mT, and particularly Bp4aT were significantly ($p < 0.001$) more active than 311 or ICL670 at inhibiting CDK2 kinase activity (Fig. 6A).

Next, we analyzed whether the inhibition of CDK2 activity parallels the inhibition of HIV-1 transcription using 293T cells. CDK2 was immunoprecipitated from 293T cells incubated with three different concentrations of Bp4eT (0.1, 1, and 10 μM), and its activity was analyzed with histone H1 as a substrate. Histone H1 phosphorylation was reduced in a dose-dependent manner, with approximately 50% inhibition at 1 μM and 85% inhibition at 10 μM (Fig. 6, B and C), being consistent with the inhibition of HIV-1 transcription (IC_{50} = 2 μM; Fig. 3A).

Inhibition of CDK9. We then analyzed whether CDK9 activity was affected in 293T cells incubated with iron chelators (all at 10 μM except ICL670A at 100 μM) for 24 h at 37°C. This was important to assess because CDK9/cyclin T1 is recruited by HIV-1 Tat to the *HIV-1* promoter and is crucial for viral replication (Nekhai and Jeang, 2006). Cyclin T1 was immunoprecipitated (Fig. 7A) and the activity of coprecipitated CDK9 was assayed with GST-CTD as a substrate. The hyperphosphorylated C-terminal domain of RNA

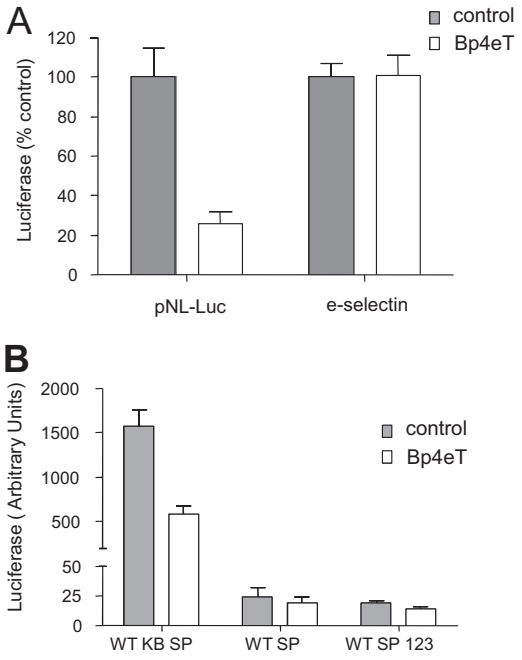

Fig. 5. Effect of Bp4eT on transcription from HIV-1 and e-selectin promoters. A, effect of iron chelators on *HIV-1* and *e-selectin* promoters. 293T cells were transiently transfected with the CMV-EGFP reporter in combination with e-selectin-luciferase (a NF-κB driven promoter), or pNL4-3.Luc.R^-E^- (*HIV-1* promoter). The cells were incubated for 24 h at 37°C in the absence or presence of Bp4eT (10 μM). The cells were lysed and the luciferase activity was measured. In parallel, EGFP fluorescence was measured and used for normalization. Values presented are mean ± S.D. ($n = 4$) in a typical experiment of two independent experiments performed. B, effect of iron chelators on basal transcription of HIV-1 LTR with deletion of NF-κB sequences and inactivation of Sp1 sites. 293T cells were transiently transfected with WT HIV-1 LTR (−105 to +77)-*luciferase* reporter (WT SP KB), HIV-1 LTR (−81 to +77) with NF-κB-deleted sites (WT SP), or HIV-1 LTR (−105 to +77) with Sp1 inactivated sites (WT SP 123). The cells were also cotransfected with the CMV-GFP expression vector. The cells were incubated with Bp4eT (10 μM) for 18 h at 37°C, then lysed and luciferase activity measured. In parallel, EGFP fluorescence was measured and used for normalization. Values presented are mean ± S.D. ($n = 4$) in a typical experiment of two independent experiments performed.

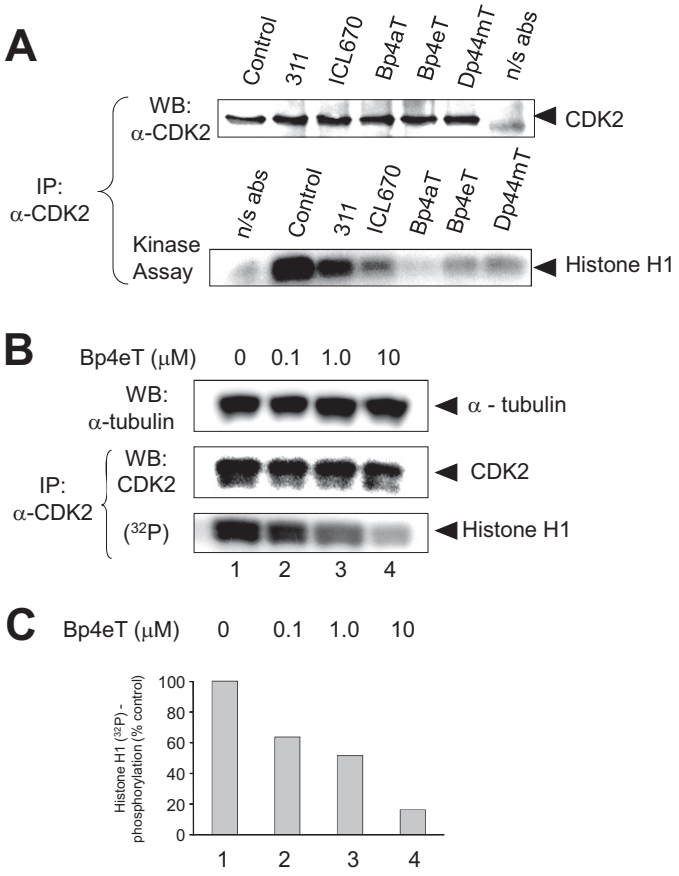

Fig. 6. Effect of iron chelators on CDK2 activity. A, inhibition of CDK2 activity by chelators. 293T cells were incubated with 311 (10 μM), ICL670 (100 μM), Bp4aT (10 μM), Bp4eT (10 μM), or Dp44mT (10 μM) for 24 h at 37°C. The cells were lysed, and CDK2 was immunoprecipitated (IP) as described under *Materials and Methods*. Top, the precipitated CDK2 was resolved on 10% SDS-PAGE and immunoblotted with antibody against CDK2. Bottom, immunoprecipitated CDK2 was used for the in vitro kinase assay using histone H1 as substrate. Phosphorylated histone H1 was resolved on SDS-PAGE and subjected to filmless autoradiographic analysis. Results presented are typical gels from three independent experiments. B, dose-dependent inhibition of CDK2 activity with Bp4eT. 293T cells were incubated with Bp4eT at concentrations of 0.1, 1.0, and 10 μM for 24 h at 37°C. Top, the level of tubulin, as a loading control, was resolved using SDS-PAGE and detected by immunoblotting. Middle, CDK2 was immunoprecipitated as described under *Materials and Methods*. The precipitated CDK2 was resolved on 10% SDS-PAGE and immunoblotted with antibody against CDK2. Bottom, CDK2 was precipitated as above and immunoprecipitated CDK2 was subsequently incubated with histone H1 in the presence of γ-(^{32}P) ATP. Kinase reactions were resolved on 10% SDS-PAGE and analyzed on a PhosphorImager. WB, Western blot. C, the density of the bands from the kinase reaction in the bottom B was quantified and presented in arbitrary units.

polymerase II (CTDo) that contains more than three phosphorylated serine residues migrates as a higher molecular weight band on SDS-PAGE (Fig. 7A). In contrast, the hypophosphorylated C-terminal domain of RNA polymerase II (CTDa), which appears as a lower molecular weight band on SDS-PAGE (Fig. 7A), comigrates with the nonphosphorylated CTD of RNA Polymerase II. CTD phosphorylation by CDK9/cyclin T1 resulted in formation of CTDo (Fig. 7A, lane 2). There was a significant ($p < 0.005$) decrease in the CTD kinase activity of CDK9/cyclin T1 in cells incubated with all the chelators (Fig. 7A).

It is noteworthy that we could not detect CDK9 that coprecipitated with cyclin T1 in cells incubated with most iron chelators, except for Bp4aT and Dp44mT, where only very faint bands were observed (Fig. 7A). Analysis of the kinase activity of CDK9 precipitated with anti-CDK9 antibody showed a marked inhibition of CDK9 activity (as demonstrated by a decrease in the intensity of the CTDo and CTDa bands) in the cells incubated with Bp4eT (10 μM) compared with untreated control cells or cells incubated with the negative control, Dp2mT (10 μM; Fig. 7B).

We then determined whether the effect of CDK9 inhibition could be due to changes in its interaction with cyclin T1 and distribution between small CDK9/cyclin T1 complexes and large CDK9/cyclin T1/HEXIM1/7SK RNA complexes. We analyzed the distribution of CDK9 and cyclin T1 between the small and large complexes using the procedure described by Biglione et al. (2007). Using this method, large and small complexes are sequentially extracted with LS and HS concentrations. Levels of CDK9 after incubating 293T cells with Bp4eT (1 μM) for 24 h at 37°C were lower than that of the control in both LS and HS extracts, whereas cyclin T1 levels were reduced only in the HS fraction (Fig. 8, A and B). These results indicate that the overall level of CDK9 expression is reduced. Furthermore, the amount of high molecular weight CDK9/cyclin T1 complex, which supplies CDK9/cyclin T1 for HIV-1 transcription (Biglione et al., 2007), was reduced after incubation with Bp4eT as demonstrated by the reduction of CDK9 in this complex (Fig. 8B).

Taken together, our data show that HIV-1 transcription is efficiently inhibited by Bp4eT- and Bp4aT-based iron chelators without apparent cytotoxicity over 24 h. This mechanism of inhibition may include the inhibition of CDK9/cyclin T1 activity, in addition to the previously shown inhibition of CDK2 activity (Debebe et al., 2007).

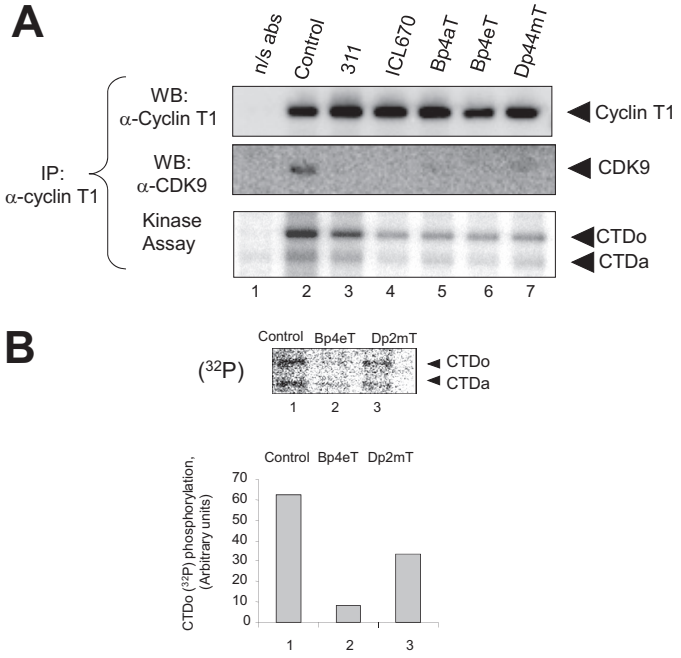

Fig. 7. Effect of iron chelators on CDK9 activity. A, inhibition of CDK9 activity. 293T cells were incubated with iron chelators (all at 10 μM except ICL670A at 100 μM) for 24 h at 37°C. The cells were lysed, and CDK9/cyclin T1 was immunoprecipitated (IP) using anti-cyclin T1 antibody. The precipitated proteins were resolved on 10% SDS-PAGE and immunoblotted with antibody against cyclin T1 (top) and CDK9 (middle) respectively. Bottom, immunoprecipitated cyclin T1 was used for the in vitro kinase assay using GST-CTD as the substrate. Phosphorylated GST-CTD was resolved by SDS-PAGE and detected using a PhosphorImager. Positions of hyper- and hypophosphorylated CTD are indicated as CTDo and CTDa. WB, Western blot. B, 293T cells were incubated with Bp4eT or Dp2mT (10 μM) for 24 h at 37°C. The cells were then lysed, and CDK9 was immunoprecipitated using anti-CDK9 antibody. Immunoprecipitated CDK9 was used for the in vitro kinase assay using GST-CTD as the substrate. Phosphorylated GST-CTD was resolved by SDS-PAGE and detected using a PhosphorImager. Positions of hyper- and hypophosphorylated CTD are indicated as CTDo and CTDa, respectively. Densitometry represents the intensity of CTDo and is presented as arbitrary units. Results presented are typical gels from three independent experiments.

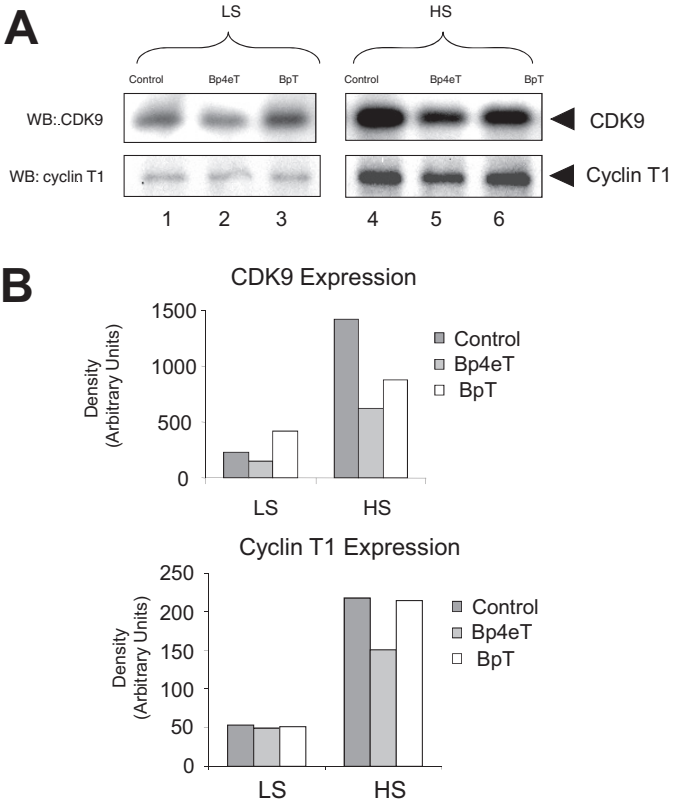

Fig. 8. Analysis of CDK9 and cyclin T1 in large and small complexes. 293T cells were incubated with Bp4eT (1 μM) for 24 h at 37°C, and CDK9/cyclin T1-containing large and small complexes were extracted using LS and HS buffers, respectively, as described under *Materials and Methods*. A, the lysates were resolved by 10% SDS-PAGE and immunoblotted using antibody against CDK9 and cyclin T1. Left, large complexes extracted with the LS buffer; right, small complexes extracted with the HS buffer. WB, Western blot. B, the intensity of the bands from A was quantified and presented in arbitrary units. Results are from a typical experiment of two performed.

Discussion

Iron is required for several steps in the HIV-1 life cycle, including reverse transcription, HIV-1 gene expression, and capsid assembly (Drakesmith and Prentice, 2008). Therefore, the use of iron chelators as a therapeutic strategy has potential and needs to be carefully assessed. Here, we focused on the effect of iron chelators on HIV-1 transcription and identified Bp4aT and Bp4eT as the two most promising agents that inhibited HIV-1 transcription in cultured cell lines and primary cells. Bp4eT was relatively nontoxic after a 24-h incubation and could be the most suitable candidate as a potential HIV-1 inhibitor. However, only Bp4aT effectively inhibited HIV-1 transcription in primary PMBCs and thus should also be further considered.

CDK2, a previously identified regulator of HIV-1 transcription (for review, see Nekhai and Jeang, 2006), was found to be a molecular target of the BpT and DpT chelators. Thus, CDK2 inhibition could be partly responsible for the antiviral activity of the chelators. Inhibition of CDK2 by either pharmacological inhibitors or CDK2-directed small interfering RNA has been shown to suppress HIV-1 replication (Agbottah et al., 2005; Ammosova et al., 2005). Iron chelators affect the activity or expression of CDK2 (Gao and Richardson, 2001; Debebe et al., 2007; Pahl et al., 2007), and deregulation of CDK2/cyclin E activity by these agents arrests cell cycle progression (Lucas et al., 1995; Pahl et al., 2000). The iron chelator desferriexochelin inhibits the binding of cyclin A and cyclin E to CDK2 in human mammary epithelial cells, whereas in human breast cancer cells, the binding is increased (Pahl et al., 2007). On the other hand, the ligand 311 inhibits the expression of cyclins D1, D2, D3, A, and B1 and also CDK2, but not cyclin E (Gao and Richardson, 2001). The chelator-mediated mechanism of inhibition of CDK2 activity may include deregulation of CDK2 binding to cyclin E or cyclin A and increased binding of the CDK inhibitor p21 to the CDK2/cyclin A complex. Considering this, iron chelators have been shown to down-regulate p21 protein expression in some cell types (Fu and Richardson, 2007) but up-regulate it in others, the effect being dependent on the cell-type assessed (R. Moussa and D. R. Richardson, unpublished data). Hence, further studies are required to assess the role of p21 in the mechanism of CDK2 inhibition by iron chelators.

In the current study, we demonstrated that the BpT- and DpT-based iron chelators can inhibit CDK2 activity. It is noteworthy that this investigation showed that in addition to the inhibition of CDK2, the chelators also inhibit CDK9/cyclin T1 activity that is recruited by HIV-1 Tat-induced HIV-1 transcription (Nekhai and Jeang, 2006). CDK9/cyclin T1 is present in cells within a large complex that contains 7SK RNA and the hexamethylene bisacetamide-induced protein and also a small complex (for review, see Michels and Bensaude, 2008). The activity of CDK9 in the large complex is inhibited by the interaction with 7SK RNA and hexamethylene bisacetamide-induced protein. The CDK9 inhibitors flavopiridol and roscovitin reduce the formation of the large complex at a concentration that inhibits HIV-1 (Biglione et al., 2007). This suggests that the large complex is important for the activation of HIV-1 transcription and may supply CDK9/cyclin T1 for Tat recruitment. We demonstrate here that CDK9/cyclin T1-kinase activity is markedly inhibited in cells incubated with Bp4aT, Bp4eT, or Dp44mT, thus providing a mechanistic explanation for the inhibitory effects of these agents on HIV-1 replication. Our analysis of the large and small complexes in the cells incubated with iron chelators showed a reduction of the CDK9, but not cyclin T1, in the high molecular weight CDK9/cyclin T1 complex. Hence, the molecular mechanism involved in preventing HIV-1 transcription by chelators could involve their targeting and inhibition of CDK9/cyclin T1 activity in addition to CDK2 activity.

HIV-1 basal transcription is largely regulated by the Sp1 transcription factor (Jochmann et al., 2009), whereas in Tat-activated transcription, NF-κB plays an important regulatory role by acting in concert with Tat and CDK9/cycin T1 (West et al., 2001). Our analysis showed that transcription from the NF-κB-dependent *e-selectin* promoter was not changed in cells incubated with Bp4eT, thus excluding NF-κB as a target for iron chelators. However, because inactivation of Sp1 as well as NF-κB sites equally decreased sensitivity of the *HIV-1* promoter to iron chelator treatment, it is possible that these agents cooperatively affect both the NF-κB and Sp1 sites. Because NF-κB acts in concert with CDK9/cyclin T1 (West et al., 2001) and Sp1 targets CDK9/cyclin T1 to the *HIV-1* promoter in the absence of Tat (Yedavalli et al., 2003), the inactivation of CDK9/cyclin T1 might affect both NF-κB and Sp1-driven transcription of the *HIV-1* promoter.

Considering the potential mechanism of the anti-HIV activity of the chelators and the possible role of CDK2 as their molecular target, it is significant to consider the following studies. CDK2 knockout mice are viable, although CDK2 is required for germ cell development, because CDK2(−/−) mice are sterile (Berthet et al., 2003). In the absence of CDK2, CDK1 compensates for its loss (Satyanarayana et al., 2008). However, the impairment of DNA repair activity makes CDK2(−/−) mice more sensitive to lethal irradiation (Satyanarayana et al., 2008). It is noteworthy that although CDK2 activity is needed for proliferation of cultured lymphocytes, proliferation of human marrow cells is driven by CDK1 combined with either cyclin A or cyclin B (Xie et al., 2008). Thus, CDK2 may be dispensable for proliferation and survival of some cells in vivo and, if so, inhibitors of CDK2 might be considered as a novel class of anti-HIV-1 therapeutics.

In addition to the inhibition of HIV-1 transcription, iron depletion may affect other steps in HIV-1 replication. During viral entry, HIV-1 replication is dependent on the activity of host cell ribonucleotide reductase that contains nonheme iron, which is important for enzymatic activity (Tsimberidou et al., 2002). Export of unspliced HIV-1 mRNA requires HIV-1 Rev protein and host elongation factor 5A (eIF5α). The eIF5α protein contains *N*-ε-4-amino-2-hydroxybutyl-lysine (hypusine) that is produced by deoxyhypusine hydroxylase, an iron-containing enzyme (Kim et al., 2006). The topical fungicide ciclopirox (which also is an iron chelator) and the orally active chelator deferiprone inhibit *HIV-1* gene expression interfering with the hydroxylation step in the hypusine modification of eIF5α (Hoque et al., 2009). Furthermore, assembly of the HIV capsid requires an ATP-binding protein, ABCE1, which contains iron-sulfur clusters (Barthelme et al., 2007) and binds to HIV-1 Gag protein (Zimmerman et al., 2002). Thus, iron chelators may have a wider spectrum of molecular targets and further studies are required to analyze these.

To assess their possible utility as pharmaceuticals against HIV-1, we compared the antiviral activity of the most efficient chelators, Bp4aT and Bp4eT, with the previously reported HIV-1 inhibitors, ARC, and roscovitin (Agbottah et al., 2005; Nekhai et al., 2007). These studies showed that the ligands were approximately 4- to 10-fold less efficient inhibitors than ARC (Fig. 3) but very similar to roscovitin. However, the fact that these chelators were not specifically designed for the treatment of HIV-1 demonstrates their clear potential. Further chemical optimization of the design of these ligands for the purpose of inhibition of HIV-1 is vital. Clearly, the good therapeutic index in short-term infectivity assays shown in the current studies must be followed with extensive in vivo assessment to ensure high tolerability, which is critical for human use (Biglione et al., 2007). Finally, it must be noted that the very different mechanism of action of these chelators compared with other established antiviral therapies is an advantage of these agents. Hence, they may be useful in terms of treating resistance to AZT and other commercially available antiviral drugs that is a major emerging problem.

Significantly, previous in vivo studies in mice examining the effects of Dp44mT have shown that it neither leads to decreased levels of tissue iron nor induces alterations in multiple hematological parameters (Yuan et al., 2004; Whitnall et al., 2006). This finding is probably due to the very low doses of the agents (0.4–0.7 mg/kg) required for efficacy. Moreover, Dp44mT was well tolerated at optimal doses, demonstrating its potential for clinical use (Yuan et al., 2004; Whitnall et al., 2006). Given the levels of cytotoxicity observed after 3 days in vitro in the current studies, questions could arise as to the feasibility of the development of these compounds as antivirals. However, many common chemotherapeutic drugs currently in clinical use (e.g., doxorubicin) display marked cytotoxicity profiles in vitro (Yuan et al., 2004) but are tolerated at appropriate doses in vivo and have led to vast improvements in a variety of disease states. Hence, clearly, the effect in vitro is difficult to directly translate to the in vivo situation and, as observed with many other drugs, appropriate dosing is key to optimizing antiviral activity and minimizing toxicity in vivo.

In conclusion, these iron chelators represent agents with a therapeutic window and novel mechanism of action that deserves further investigation in terms of their use in future anti-HIV-1 therapeutic regimens. Their potential may be particularly significant where resistance to standard antiviral therapy occurs.

Acknowledgments

We acknowledge Dr. Anna Suter (Novartis, Pharma AG, Ltd., Basel, Switzerland) for ICL670. We appreciate the assistance of Keon Combi, Xiomei Niu, and Dillon Robinson in cell counting and toxicity assays. We are also thankful to Dr. Kuan-Teh Jeang (National Institute of Allergy and Infectious Diseases, National Institutes of Health) for critical reading and comments on the manuscript. Finally, Dr. Katie Dixon, Zaklina Kovacevic, and Dr. Helena Mangs (Iron Metabolism and Chelation Program, University of Sydney, Sydney, Australia) are acknowledged for thorough assessment of the manuscript.

Authorship Contributions

Participated in research design: Debebe, Ammosova, Breuer, Jerebtsova, Kashanchi, and Nekhai

Conducted experiments: Debebe, Ammosova, Breuer, Kashanchi, and Nekhai.

Contributed new reagents or analytic tools: Lovejoy, Kalinowski, Jerebtsova, Ray, and Richardson.

Performed data analysis: Debebe, Ammosova, Breuer, and Nekhai.

Wrote or contributed to the writing of the manuscript: Debebe, Gordeuk, Kalinowski, Lovejoy, Richardson, and Nekhai.

Other: Debebe, Gordeuk, Kalinowski, Lovejoy, Richardson, and Nekhai acquired funding for the research.

References

Agbottah E, de La Fuente C, Nekhai S, Barnett A, Gianella-Borradori A, Pumfery A, and Kashanchi F (2005) Antiviral activity of CYC202 in HIV-1-infected cells. *J Biol Chem* **280:**3029–3042.

Ammosova T, Berro R, Kashanchi F, and Nekhai S (2005) RNA interference directed to CDK2 inhibits HIV-1 transcription. *Virology* **341:**171–178.

Barthelme D, Scheele U, Dinkelaker S, Janoschka A, Macmillan F, Albers SV, Driessen AJ, Stagni MS, Bill E, Meyer-Klaucke W, et al. (2007) Structural organization of essential iron-sulfur clusters in the evolutionarily highly conserved ATP-binding cassette protein ABCE1. *J Biol Chem* **282:**14598–14607.

Becker EM, Lovejoy DB, Greer JM, Watts R, and Richardson DR (2003) Identification of the di-pyridyl ketone isonicotinoyl hydrazone (PKIH) analogues as potent iron chelators and anti-tumour agents. *Br J Pharmacol* **138:**819–830.

Berthet C, Aleem E, Coppola V, Tessarollo L, and Kaldis P (2003) Cdk2 knockout mice are viable. *Curr Biol* **13:**1775–1785.

Biglione S, Byers SA, Price JP, Nguyen VT, Bensaude O, Price DH, and Maury W (2007) Inhibition of HIV-1 replication by P-TEFb inhibitors DRB, seliciclib and flavopiridol correlates with release of free P-TEFb from the large, inactive form of the complex. *Retrovirology* **4:**47.

Butera ST, Roberts BD, Lam L, Hodge T, and Folks TM (1994) Human immunodeficiency virus type 1 RNA expression by four chronically infected cell lines indicates multiple mechanisms of latency. *J Virol* **68:**2726–2730.

Chun RF, Semmes OJ, Neuveut C, and Jeang KT (1998) Modulation of Sp1 phosphorylation by human immunodeficiency virus type 1 Tat. *J Virol* **72:**2615–2629.

Debebe Z, Ammosova T, Jerebtsova M, Kurantsin-Mills J, Niu X, Charles S, Richardson DR, Ray PE, Gordeuk VR, and Nekhai S (2007) Iron chelators ICL670 and 311 inhibit HIV-1 transcription. *Virology* **367:**324–333.

Drakesmith H and Prentice A (2008) Viral infection and iron metabolism. *Nat Rev Microbiol* **6:**541–552.

Fu D and Richardson DR (2007) Iron chelation and regulation of the cell cycle: 2 mechanisms of posttranscriptional regulation of the universal cyclin-dependent kinase inhibitor p21CIP1/WAF1 by iron depletion. *Blood* **110:**752–761.

Fu DX, Kuo YL, Liu BY, Jeang KT, and Giam CZ (2003) Human T-lymphotropic virus type I tax activates I-kappa B kinase by inhibiting I-kappa B kinase-associated serine/threonine protein phosphatase 2A. *J Biol Chem* **278:**1487–1493.

Gao J and Richardson DR (2001) The potential of iron chelators of the pyridoxal isonicotinoyl hydrazone class as effective antiproliferative agents, IV: The mechanisms involved in inhibiting cell-cycle progression. *Blood* **98:**842–850.

Georgiou NA, van der Bruggen T, Oudshoorn M, Hider RC, Marx JJ, and van Asbeck BS (2002) Human immunodeficiency virus type 1 replication inhibition by the bidentate iron chelators CP502 and CP511 is caused by proliferation inhibition and the onset of apoptosis. *Eur J Clin Invest* **32 (Suppl 1):**91–96.

Georgiou NA, van der Bruggen T, Oudshoorn M, Nottet HS, Marx JJ, and van Asbeck BS (2000) Inhibition of human immunodeficiency virus type 1 replication in human mononuclear blood cells by the iron chelators deferoxamine, deferiprone, and bleomycin. *J Infect Dis* **181:**484–490.

Gómez-Gonzalo M, Carretero M, Rullas J, Lara-Pezzi E, Aramburu J, Berkhout B, Alcamí J, and López-Cabrera M (2001) The hepatitis B virus X protein induces HIV-1 replication and transcription in synergy with T-cell activation signals: functional roles of NF-kappaB/NF-AT and SP1-binding sites in the HIV-1 long terminal repeat promoter. *J Biol Chem* **276:**35435–35443.

Gordeuk VR, Delanghe JR, Langlois MR, and Boelaert JR (2001) Iron status and the outcome of HIV infection: an overview. *J Clin Virol* **20:**111–115.

He J and Landau NR (1995) Use of a novel human immunodeficiency virus type 1 reporter virus expressing human placental alkaline phosphatase to detect an alternative viral receptor. *J Virol* **69:**4587–4592.

Hershko C (1994) Control of disease by selective iron depletion: a novel therapeutic strategy utilizing iron chelators. *Baillieres Clin Haematol* **7:**965–1000.

Hoque M, Hanauske-Abel HM, Palumbo P, Saxena D, D'Alliessi Gandolfi D, Park MH, Pe'ery T, and Mathews MB (2009) Inhibition of HIV-1 gene expression by Ciclopirox and Deferiprone, drugs that prevent hypusination of eukaryotic initiation factor 5A. *Retrovirology* **6:**90.

Jochmann R, Thurau M, Jung S, Hofmann C, Naschberger E, Kremmer E, Harrer T, Miller M, Schaft N, and Stürzl M (2009) O-linked N-acetylglucosaminylation of Sp1 inhibits the human immunodeficiency virus type 1 promoter. *J Virol* **83:**3704–3718.

Kalinowski DS, Yu Y, Sharpe PC, Islam M, Liao YT, Lovejoy DB, Kumar N, Bernhardt PV, and Richardson DR (2007) Design, synthesis, and characterization of novel iron chelators: structure-activity relationships of the 2-benzoylpyridine thiosemicarbazone series and their 3-nitrobenzoyl analogues as potent antitumor agents. *J Med Chem* **50:**3716–3729.

Kim YS, Kang KR, Wolff EC, Bell JK, McPhie P, and Park MH (2006) Deoxyhypusine hydroxylase is a Fe(II)-dependent, HEAT-repeat enzyme. Identification of amino acid residues critical for Fe(II) binding and catalysis [corrected]. *J Biol Chem* **281:**13217–13225.

Lucas JJ, Szepesi A, Domenico J, Takase K, Tordai A, Terada N, and Gelfand EW (1995) Effects of iron-depletion on cell cycle progression in normal human T

lymphocytes: selective inhibition of the appearance of the cyclin A-associated component of the p33cdk2 kinase. *Blood* **86:**2268–2280.
Michels AA and Bensaude O (2008) RNA-driven cyclin-dependent kinase regulation: when CDK9/cyclin T subunits of P-TEFb meet their ribonucleoprotein partners. *Biotechnol J* **3:**1022–1032.
Nekhai S, Bhat UG, Ammosova T, Radhakrishnan SK, Jerebtsova M, Niu X, Foster A, Layden TJ, and Gartel AL (2007) A novel anticancer agent ARC antagonizes HIV-1 and HCV. *Oncogene* **26:**3899–3903.
Nekhai S and Jeang KT (2006) Transcriptional and post-transcriptional regulation of HIV-1 gene expression: role of cellular factors for Tat and Rev. *Future Microbiol* **1:**417–426.
Pahl PM, Reese SM, and Horwitz LD (2007) A lipid-soluble iron chelator alters cell cycle regulatory protein binding in breast cancer cells compared to normal breast cells. *J Exp Ther Oncol* **6:**193–200.
Pahl PM, Yan XD, Hodges YK, Rosenthal EA, Horwitz MA, and Horwitz LD (2000) An exochelin of Mycobacterium tuberculosis reversibly arrests growth of human vascular smooth muscle cells in vitro. *J Biol Chem* **275:**17821–17826.
Papadopoulos NG, Dedoussis GV, Spanakos G, Gritzapis AD, Baxevanis CN, and Papamichail M (1994) An improved fluorescence assay for the determination of lymphocyte-mediated cytotoxicity using flow cytometry. *J Immunol Methods* **177:** 101–111.
Porter JB (2006) Deferasirox: An effective once-daily orally active iron chelator. *Drugs Today (Barc)* **42:**623–637.
Satyanarayana A, Hilton MB, and Kaldis P (2008) p21 Inhibits Cdk1 in the absence of Cdk2 to maintain the G1/S phase DNA damage checkpoint. *Mol Biol Cell* **19:**65–77.
Traoré HN and Meyer D (2004) The effect of iron overload on in vitro HIV-1 infection. *J Clin Virol* **31 (Suppl 1):**S92–S98.
Tsimberidou AM, Alvarado Y, and Giles FJ (2002) Evolving role of ribonucleoside reductase inhibitors in hematologic malignancies. *Expert Rev Anticancer Ther* **2:**437–448.
West MJ, Lowe AD, and Karn J (2001) Activation of human immunodeficiency virus transcription in T cells revisited: NF-kappaB p65 stimulates transcriptional elongation. *J Virol* **75:**8524–8537.
Whitnall M, Howard J, Ponka P, and Richardson DR (2006) A class of iron chelators with a wide spectrum of potent antitumor activity that overcomes resistance to chemotherapeutics. *Proc Natl Acad Sci USA* **103:**14901–14906.
Xie DX, Yao J, Zhang P, Li XL, Feng YD, Wu JH, Tao DD, Hu JB, and Gong JP (2008) Are progenitor cells pre-programmed for sequential cell cycles not requiring cyclins D and E and activation of Cdk2? *Cell Prolif* **41:**265–278.
Yedavalli VS, Benkirane M, and Jeang KT (2003) Tat and trans-activation-responsive (TAR) RNA-independent induction of HIV-1 long terminal repeat by human and murine cyclin T1 requires Sp1. *J Biol Chem* **278:**6404–6410.
Yuan J, Lovejoy DB, and Richardson DR (2004) Novel di-2-pyridyl-derived iron chelators with marked and selective antitumor activity: in vitro and in vivo assessment. *Blood* **104:**1450–1458.
Zimmerman C, Klein KC, Kiser PK, Singh AR, Firestein BL, Riba SC, and Lingappa JR. Identification of a host protein essential for assembly of immature HIV-1 capsids. *Nature* **415(6867):**88–92, 2002.

Address correspondence to: Sergei Nekhai, Center for Sickle Cell Disease, Howard University, 1840 7th St. N.W., HURB1, Suite 202, Washington DC 20001. E-mail: snekhai@howard.edu